THE JOURNAL OF BIOLOGICAL CHEMISTRY
Vol. 255, No. 9, Issue of May 10, pp. 4100–4111, 1980
Printed in U.S.A.

On the Mechanism of Action of Cytochrome P-450

SPECTRAL INTERMEDIATES IN THE REACTION OF P-450$_{LM_2}$ WITH PEROXY COMPOUNDS*

(Received for publication, December 10, 1979)

Robert C. Blake II‡ and Minor J. Coon

From the Department of Biological Chemistry, Medical School, The University of Michigan, Ann Arbor, Michigan 48109

In previous studies in this laboratory, highly purified liver microsomal cytochrome P-450 was shown to catalyze the hydroperoxide-dependent hydroxylation of a variety of substrates in the absence of NADPH, NADPH-cytochrome P-450 reductase, and molecular oxygen, and evidence was obtained that the oxygen atom in the product was derived from the peroxide. To determine whether the cytochrome functions in such reactions by a peroxidase-type mechanism, the kinetics of its interactions with a variety of substituted hydroperoxides and peroxy acids have been determined by stopped flow spectrophotometry.

The reaction of P-450$_{LM_2}$ with various peroxy compounds yields an intermediate with an absorption maximum at about 436 nm in the difference spectrum, with pseudo-first order or biphasic kinetics depending upon the individual rate constants and the concentration of the oxidant used. The results are in accord with a reversible two-step mechanism, as follows:

$$\text{P-450} + \text{oxidant} \rightleftharpoons \text{C} \rightleftharpoons \text{D},$$

where C represents a transient intermediate which is detected spectrally only under certain conditions and is probably an enzyme•oxidant complex, and D is the complex with an absorption maximum at about 436 nm in the difference spectrum. The absolute and difference spectra of C and D vary in magnitude and in the positions of maxima and minima with the organic moiety of the peroxy compound used. Whereas the kinetics of the reaction with cumene hydroperoxide and benzyl hydroperoxide is unchanged in the pH range 5.0 to 9.0, that of perbenzoic acids decreases markedly at higher pH, thus indicating that only the unionized compound reacts with the enzyme. Experiments with a variety of substituted cumene hydroperoxides, benzyl hydroperoxides, and perbenzoic acids indicated that the first equilibrium is driven to the right by hydrophobic bonding of the oxidant to P-450$_{LM_2}$ and that the rate of conversion of C to D is increased by electron-withdrawing substituents in the oxidant and decreased by electron-donating substituents. Following the formation of Complex D, irreversible heme destruction occurs slowly.

These results indicate that the reaction of liver microsomal P-450 with peroxides differs in two important respects from that of typical peroxidases; the intermediates arising from the reaction of P-450$_{LM_2}$ with peroxy compounds are formed reversibly, and the spectra of these intermediates vary with structural differences in the peroxy compounds. Furthermore, the absence of a common isosbestic point in the spectra observed with P-450$_{LM_2}$ rules out the possibility that they represent mixtures of Compounds I and II as reported for peroxidases.

Studies in many laboratories have shown that liver microsomal cytochrome P-450 catalyzes the hydroxylation of a variety of physiologically occurring lipids and foreign compounds. The stoichiometry of the overall process was studied in a reconstituted enzyme system containing cytochrome P-450, NADPH-cytochrome P-450 reductase, and phosphatidylcholine (3–6) and found to represent the sum of two activities (7). These are the hydroxylation reaction itself,

$$\text{RH} + \text{O}_2 + \text{NADPH} + \text{H}^+ \rightarrow \text{ROH} + \text{H}_2\text{O} + \text{NADP}^+, \quad (1)$$

where RH represents the substrate and ROH the product, and an oxidase activity apparently resulting from autoxidation of the reduced cytochrome in the presence of oxygen,

$$\text{O}_2 + \text{NADPH} + \text{H}^+ \rightarrow \text{H}_2\text{O}_2 + \text{NADP}^+. \quad (2)$$

In addition, P-450$_{LM}$[1] is able to catalyze the oxidation of organic substrates at the expense of peroxy compounds. This reaction, first shown with drugs and cumene hydroperoxide in microsomal suspensions by Kadlubar *et al.* (8) and Rahimtula and O'Brien (9), occurs with a number of oxidants other than alkyl hydroperoxides, such as peroxy acids (10), sodium periodate (11), sodium chlorite (10), iodosobenzene (12, 13), iodosobenzene diacetate (13, 14), and pyridine *N*-oxide (15). This laboratory (10) showed several years ago that electrophoretically homogeneous P-450$_{LM_2}$ catalyzes such reactions in the absence of NADPH, NADPH-cytochrome P-450 reductase, and molecular oxygen and that the reaction has the following stoichiometry:

$$\text{RH} + \text{R'OOH} \rightarrow \text{ROH} + \text{R'OH}, \quad (3)$$

where RH and ROH again represent the substrate and product, respectively, and R'OOH represents the peroxy compound serving as the oxygen donor (for example, cumene hydroperoxide) and R'OH the corresponding decomposition product (for example, cumenol). Phosphatidylcholine is required for

* This research was supported by Grant AM-10339 from the United States Public Health Service and Grant PCM76-14947 from the National Science Foundation. Preliminary reports of part of this investigation have been presented (1, 2). The costs of publication of this article were defrayed in part by the payment of page charges. This article must therefore be hereby marked "*advertisement*" in accordance with 18 U.S.C. Section 1734 solely to indicate this fact.

‡ Recipient of a National Research Service Award from the National Institutes of Health.

[1] The abbreviations used are: P-450$_{LM}$, liver microsomal cytochrome P-450; dilauroyl-GPC, dilauroylglyceryl-3-phosphorylcholine; and CHP, cumene hydroperoxide. The isozymes of liver microsomal cytochrome P-450 are numbered according to their relative electrophoretic mobilities when submitted to sodium dodecyl sulfate-polyacrylamide gel electrophoresis; P-450$_{LM_2}$ is the isozyme induced by phenobarbital.

maximal rates of substrate hydroxylation in Reaction 3 as well as in Reaction 1.

The present paper is concerned with the question of whether such peroxide-supported reactions occur by a classical peroxidase-type mechanism. As reviewed elsewhere (16, 17), the possibility may be considered that such a mechanism applies as well to the O_2-supported reactions, in which molecular oxygen is reduced to hydrogen peroxide. Oxidation reactions mediated by known peroxidases involve the intermediate formation of an oxygen derivative called Compound I, as follows:

$$\underset{\text{(Native enzyme)}}{(Fe)^{3+}} + R'OOH \rightarrow \underset{\text{(Compound I)}}{(Fe\text{-}O)^{3+}} + R'OH, \quad (4)$$

in which $(Fe\text{-}O)^{3+}$ represents an iron-coordinated oxygen complex of unspecified electron distribution having a formal oxidation state of +5. Preliminary experiments indicated that the reaction of *m*-chloroperbenzoic acid with purified P-450$_{LM_2}$ yields an intermediate with absorption maxima at 375, 421, and 540 nm in the absolute spectrum and at 370, 438, and 540 nm in the difference spectrum (intermediate minus native, ferric cytochrome) (2). This difference spectrum is similar to that observed with this peracid in liver microsomal suspensions by Lichtenberger and Ullrich (12, 18), and the difference spectrum observed with cumene hydroperoxide and P-450$_{LM_2}$ is similar to that observed in liver microsomal suspensions by Rahimtula *et al.* (19) and Hrycay *et al.* (20). The stopped flow spectrophotometric studies to be described involving purified P-450$_{LM_2}$ and a series of perbenzoic acids, cumene hydroperoxides, and benzyl hydroperoxides gave no indication that a Compound I-like intermediate was formed. The spectral intermediates observed differed in two important respects from those predicted by Reaction 4; with P-450$_{LM_2}$ the reaction with peroxides is reversible, and the spectra vary with the organic structure of the peroxy compound studied.

EXPERIMENTAL PROCEDURES

Purification of Cytochrome P-450—P-450$_{LM_2}$ was prepared from hepatic microsomes of phenobarbital-induced rabbits according to published procedures (21–23). The concentration of P-450$_{LM_2}$ was determined from the absorbance at 451 nm in the absolute spectrum of the ferrous·carbonyl complex using an extinction coefficient of 110 mM^{-1} cm^{-1} (22). The preparations used in these experiments had specific contents of 14.2 to 18.9 nmol of P-450$_{LM_2}$ per mg of protein and gave a single major band upon sodium dodecyl sulfate-polyacrylamide gel electrophoresis.

Stopped Flow Measurements—Stopped flow spectrophotometry was performed with an instrument designed and constructed in this laboratory by Mr. Shaun D. Black and Dr. David P. Ballou. Unless otherwise noted, the P-450$_{LM_2}$ and the peroxy compound were prepared in 0.05 M sodium phosphate buffer, pH 7.0, and added to separate syringes of the stopped flow spectrophotometer. The P-450$_{LM_2}$ solution contained sonicated dilauroyl-GPC at a concentration of 100 μg per ml. The temperature of the mixing chamber and the driving syringes was maintained at 10 ± 0.1°C by circulating water. Reactions were initiated by rapidly mixing 0.1 ml of the solution·from each driving syringe. Spectral changes, which were observed through a 2-cm optical path length, were linear to an absorbance of 1.8. A 3.0-nm spectral band width was used, as this produced acceptable signal to noise characteristics.

Synthesis of Peroxy Compounds—All of the perbenzoic acids except *p-n*-propylperbenzoic acid were prepared by the alkaline perhydrolysis of the corresponding benzoyl chlorides in the presence of magnesium sulfate (24). Two minor modifications of the published procedure were employed to improve both the yield and the purity of the peracid. The yield was substantially improved by maintaining the temperature of the reaction mixture below 8°C, rather than 25°C. Since the major impurity in the perbenzoic acid reaction mixture was the corresponding benzoic acid, the two compounds were separated on the basis of their pK_a differences. After extraction of the crude product into cold methylene chloride, the benzoic acid was extracted into 0.2 M sodium phosphate buffer, pH 6.0. The methylene chloride layer (containing the unionized perbenzoic acid) was then dried over anhydrous magnesium sulfate, and the solvent was removed on a rotary evaporator under a full vacuum attained with an oil pump and dry ice trap. Care was taken to keep the temperature of the rotary evaporator bath below 5°C.

When the acid and peracid were very hydrophobic (as with *p-n*-propyl- and *p-t*-butylperbenzoic acids and 2-pernaphthoic acid), the procedure for extracting the contaminating acid was ineffective, and peracids of unacceptable purity were obtained. An alternative synthesis (25) employing *p-n*-propylbenzoic acid, methane sulfonic acid, and 90% H_2O_2 was, therefore, used to prepare *p-n*-propylperbenzoic acid of 88% purity. Attempts to synthesize *p-t*-butylperbenzoic acid and 2-pernaphthoic acid by this procedure resulted in a violent decomposition of the organic acid.

Benzyl hydroperoxides were prepared from the appropriate benzyl bromide or iodide and 90% H_2O_2 in the presence of silver trifluoroacetate as stated without detail by Cookson *et al.* (26). The benzyl iodide, which was used whenever an electron-withdrawing group was present as a ring substituent, was prepared by treating the corresponding benzyl bromide with NaI in acetone until precipitation of NaBr was complete. An ethyl ether solution (20 ml) containing 2.4 g of silver trifluoroacetate was added dropwise to a rapidly stirred solution of ethyl ether (10 ml) containing 0.01 mol of the benzyl halide and 4 ml of 90% H_2O_2. The reaction mixture was kept below 5°C in an ice bath. When precipitation of the silver halide was complete, the precipitate was removed by filtration, and the trifluoroacetic acid and the excess H_2O_2 were removed by treatment of the solution with aqueous sodium bicarbonate (0.1 M). The solvent was then removed in a rotary evaporator, and the residual crude hydroperoxide was purified by the same procedure used to purify commercial cumene hydroperoxide (27).

The cumene hydroperoxides were prepared by a three-step synthesis starting from the appropriate *m*- and *p*-substituted acetophenone, which was converted to the corresponding α,α-dimethylbenzyl alcohol (hereafter referred to as cumenol) by a Grignard reaction with methyl iodide. The cumenol was converted to either the cumyl chloride or cumyl bromide by dissolving the alcohol in methylene chloride and passing HCl or HBr through the solution (28). The hydroperoxide was then prepared from the alkyl halide and purified using the procedures described above for the synthesis of the benzyl hydroperoxides. All of the purified peroxy compounds were stored at −20°C in polypropylene vials.

The purity of the benzyl and cumene hydroperoxides was determined by iodometric titration using a published procedure (29). With peroxy acids the same method was used, but without heating. Such titrations indicated that the purity of the resulting peracids, benzyl hydroperoxides, and cumene hydroperoxides was in all cases greater than 93, 90, and 87%, respectively. The remaining material was predominantly the corresponding carboxylic acid in the peracids, as shown by nmr analysis, and the corresponding alcohol in the hydroperoxides, as shown by nmr and ir analysis of occasional samples.

Materials—The substituted benzoyl chlorides, benzyl bromides or iodides, and acetophenones used to synthesize the various peroxy compounds were obtained from four commercial sources: Sigma, Aldrich Chemical Co., Pfaltz and Bauer, and Eastman Organic Chemicals. All these starting materials were reagent grade and were used without further purification. Thirty per cent and ninety per cent H_2O_2 were obtained from Mallinckrodt and FMC Corporation, respectively. Cumene hydroperoxide was purchased from K and K Laboratories and purified by published procedures (27), and dilauroyl-GPC was obtained from Serdary Research Laboratories. All other chemicals were reagent grade.

RESULTS

When purified P-450$_{LM_2}$ was mixed in a stopped flow spectrophotometer with any one of a variety of *m*- or *p*-substituted aromatic peroxy compounds, the absorbance changed with time in either a pseudo-first order or biphasic manner. A representative example of each type of kinetic behavior is discussed below. Each example illustrates the general approach taken to recognize the minimal kinetic mechanism that could account for the observed spectral changes and to obtain the values of the relevant rate constants. Thus, each example serves as a model for the other peroxy compounds which produced the same kind of absorbance changes.

Pseudo-First Order Absorbance Changes—Fig. 1*A* illus-

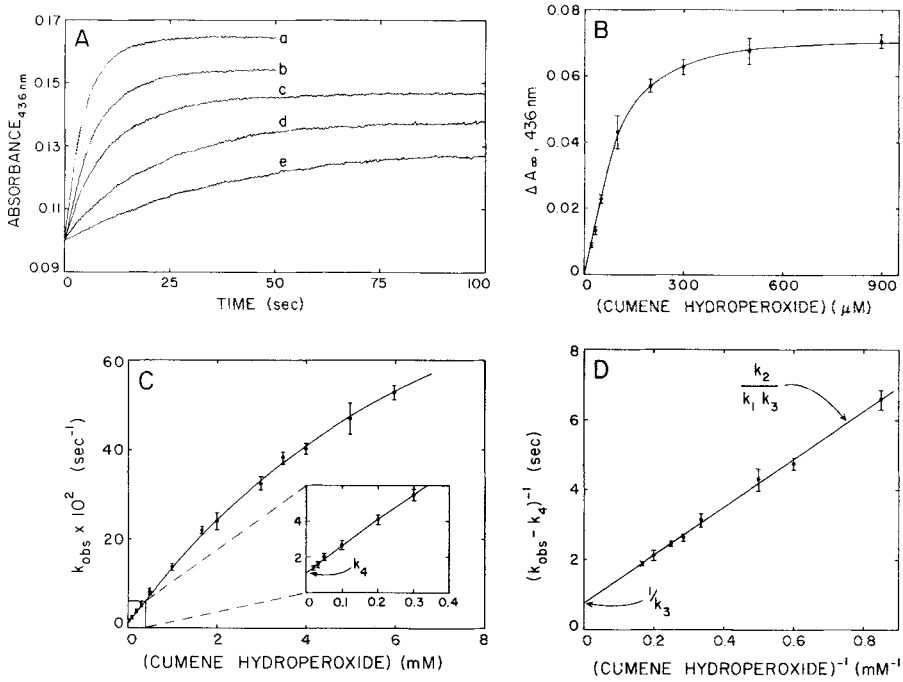

FIG. 1. **Calculation of rate constants when the kinetic traces were pseudo-first order.** *A*, shows representative stopped flow kinetic traces observed at 436 nm after P-450$_{LM_2}$ was mixed with different concentrations of cumene hydroperoxide. The final concentrations after mixing were: P-450$_{LM_2}$, 2.8 μM; cumene hydroperoxide, 1000, 300, 200, 100, and 50 μM in Experiments *a* through *e*, respectively. *B*, shows the dependence of the total absorbance change, ΔA_∞, upon the final concentration of cumene hydroperoxide. The absorbance changes in *A* and *B* are those observed with a 2-cm optical path length. *C*, shows the dependence of the pseudo-first order rate constant, k_{obs}, for the absorbance change at 436 nm upon the final concentration of cumene hydroperoxide. *Inset*, an expansion of the results at the lowest cumene hydroperoxide concentrations. The values of both k_{obs} and ΔA_∞ were obtained as described in the text. *D*, shows a linear plot, according to Equation 9 in the text, of the reciprocal of $(k_{obs} - k_4)$ *versus* the reciprocal of the cumene hydroperoxide concentration. The ordinate intercept and slope were determined by a linear regression analysis. Each *error bar* in parts *B*, *C*, and *D* represents the standard deviation of eight determinations. The *lines* drawn through the data points and the standard deviations shown in parts *C* and *D* were generated assuming the applicability of Equations 8 and 9 and using the values for the rate constants listed in Table I.

trates the typical pseudo-first order behavior observed when P-450$_{LM_2}$ was mixed with different concentrations of cumene hydroperoxide. Each kinetic trace obtained with cumene hydroperoxide could be described mathematically as a single exponential function of time:

$$\Delta A_t = \Delta A_\infty e^{-k_{obs}t} \tag{5}$$

where ΔA_t is the absorbance at the end of the reaction minus the absorbance at time t ($A_\infty - A_t$), ΔA_∞ is the total absorbance change observed ($A_\infty - A_0$), and k_{obs} is the observed pseudo-first order rate constant for the absorbance change. Accurate values of both ΔA_∞ and k_{obs} were obtained from the ordinate intercepts and slopes, respectively, of semilogarithmic plots of ΔA_t *versus* time. These values were then used in subsequent secondary plots. No discernible lags were observed in these semilogarithmic plots, which were linear to greater than four half-lives of the reaction.

It is clear from Fig. 1*A* that both the rate and the amplitude of the absorbance changes are functions of the cumene hydroperoxide concentration. The plot in Fig. 1*B* shows the dependence of the total absorbance change, ΔA_∞, upon the concentration of cumene hydroperoxide. It should be noted that this dependence does not represent a stoichiometric titration of P-450 (2.8 μM) with cumene hydroperoxide. On the contrary, the value of ΔA_∞ was observed to be a hyperbolic function of the concentration of the oxidant:

$$\Delta A_\infty = \frac{\Delta A'_\infty\,(\mathrm{CHP})}{(\mathrm{CHP}) + K_d} \tag{6}$$

where $\Delta A'_\infty$ is the ΔA_∞ at infinite (CHP), and K_d is the apparent dissociation constant for the cumene hydroperoxide. Thus, a Benesi-Hildebrand plot (30) of ΔA_∞^{-1} *versus* $(\mathrm{CHP})^{-1}$ yielded a linear plot (not shown) from which $\Delta A'_\infty$ and K_d (73 μM) were calculated.

The dependence of k_{obs} upon the concentration of cumene hydroperoxide, which was varied over a 300-fold range, is shown in Fig. 1*C*. The value of k_{obs} was observed to be a nonlinear, concave-down function of the cumene hydroperoxide concentration with a positive ordinate intercept. The kinetic behavior reflected in parts *A*, *B*, and *C* of Fig. 1 has been shown to be diagnostic for the following simple mechanism (31):

$$\mathrm{A} + \mathrm{B} \underset{k_2}{\overset{k_1}{\rightleftharpoons}} \mathrm{C} \underset{k_4}{\overset{k_3}{\rightleftharpoons}} \mathrm{D} \tag{7}$$

where A is the native P-450$_{LM_2}$, B is the peroxy compound (in this case, cumene hydroperoxide), and Complexes C and D represent two distinct species with Complex D being the species that is monitored. Application of the rapid equilibrium assumption ($k_2 \gg k_3$) to species C gives the following expression for k_{obs} for the appearance of Complex D as a function of the cumene hydroperoxide concentration and the individual rate constants (31):

$$k_{obs} = \frac{k_1k_3(\mathrm{CHP})}{k_1(\mathrm{CHP}) + k_2} + k_4 \tag{8}$$

A value of $k_4 = 0.011\ s^{-1}$ was thus obtained from the ordinate intercept of Fig. 1*C*. With this value of k_4, a double reciprocal plot of $(k_{obs} - k_4)^{-1}$ *versus* $(\mathrm{CHP})^{-1}$ should generate a linear plot according to the expression,

$$\frac{1}{(k_{obs} - k_4)} = \frac{1}{k_3} + \frac{k_2}{k_1k_3(\mathrm{CHP})} \tag{9}$$

This plot is illustrated in Fig. 1*D*; values of $k_3 = 1.5\ s^{-1}$ and $k_2/k_1 = 10$ mM were calculated from the ordinate intercept and slope, respectively. Individual values for k_1 and k_2 could be estimated by employing an additional equation which describes the behavior in Fig. 1*B*, but a more reliable method of determining these values is discussed below.

Since k_{obs} was independent of the wavelength being monitored, a similar analysis of data collected at 415 nm (where the absorbance of the P-450 decreases with time) produced the same values for the various rate constants as those determined at 436 nm. These experimental results were very reproducible. Variations in the specific content of the enzyme preparation or the purity of the cumene hydroperoxide (83% as compared to the 97% pure material usually used) had no appreciable effect on the experimental observations. Likewise, the presence or absence of phospholipid had no apparent effect on the kinetic behavior or spectral changes. As long as pseudo-first order conditions were maintained, protein concentrations from 1.1 μM to 7.8 μM affected only the amplitude of the observed spectral changes, not the k_{obs}. The amplitudes were directly proportional to the concentration of P-450.

The behavior observed when P-450$_{LM_2}$ is exposed to cumene hydroperoxide can thus be characterized mathematically by a mechanism involving two consecutive equilibria. The first equilibrium involves a bimolecular combination of free P-450 and cumene hydroperoxide to form Complex C (which has a dissociation constant of 10 mM) and is established rapidly compared to the second equilibrium. The second equilibrium involves a unimolecular conversion of Complex C to Complex D, and favors the latter by a 136:1 ratio. At cumene hydroperoxide concentrations very much greater than 10 mM, most of the free P-450 should be rapidly converted to Complex C according to the first equilibrium. This high concentration of Complex C would then be transformed almost completely to Complex D with an apparent first order rate constant approaching $1.5\ s^{-1}$ at an infinitely high concentration of cumene hydroperoxide. The formation and subsequent decay of Complex C should be directly observable; however, the formation of Complex C would be expected to occur in the dead time of the stopped flow spectrophotometer.

At cumene hydroperoxide concentrations much less than 10 mM, only a very small amount of the free P-450 should be rapidly converted to Complex C in the first equilibrium. Since the overall dissociation constant for Complex D to form P-450$_{LM_2}$ and peroxy compound is so much less than the dissociation constant for Complex C, significant levels of Complex D can be formed even though the concentration of Complex C never exceeds more than a few per cent of the total enzyme concentration. Therefore, the reaction will appear experimentally to be a unimolecular conversion of free P-450 to Complex D with a pseudo-first order rate constant approaching $0.011\ s^{-1}$ at very low concentrations of cumene hydroperoxide. In this case, Complex C would probably not be detected directly, although its existence could be deduced kinetically. This is precisely the situation obtained with cumene hydroperoxide concentrations less than approximately 1.0 mM. Although the conversion to the spectral intermediate called Complex D appears pseudo-first order (Fig. 1*A*), the kinetic behavior indicates the existence of another intermediate prior to Complex D formation (Fig. 1, *C* and *D*). At cumene hydroperoxide concentrations below 1.0 mM, the absorbance of the P-450 at 426 nm, an isosbestic point between native P-450 and Complex D, appeared unchanged over the time course of Complex D formation (not shown). At cumene hydroperoxide concentrations of 1.0 mM or greater, the absorbance of the P-450 at 426 nm underwent a small, but nonetheless reproducible, change on a very fast time scale relative to Complex D formation. This change could be attributed to transient formation of Complex C. The absorbance at 426 nm then decayed back to its approximate starting value with a pseudo-first order rate constant equal to k_{obs}. The amplitude of this transient change in absorbance increased with increasing concentrations of cumene hydroperoxide. Since this first equilibrium is established quite rapidly compared to the second, the two equilibria can be considered uncoupled, and the transient formation of Complex C can be approximated by the simple equation,

$$\text{P-450}_{LM_2} + \text{cumene hydroperoxide} \underset{k_2}{\overset{k_1}{\rightleftharpoons}} \text{Complex C} \qquad (10)$$

Under pseudo-first order conditions, the formation of Complex C will appear first order with an apparent rate constant as follows (32):

$$k_{obs} = k_1(\text{CHP}) + k_2 \qquad (11)$$

A plot of k_{obs} for the appearance of this transient species *versus* the concentration of cumene hydroperoxide was linear over the concentration range of 1.0 to 6.0 mM cumene hydroperoxide (not shown). Values of $k_1 = 5000\ M^{-1}s^{-1}$ and $k_2 = 50\ s^{-1}$ were calculated from this plot. Note that the value calculated for k_2 is, as expected, very much greater than that determined for k_3; thus, the equilibrium assumption made above was valid. Above 6.0 mM cumene hydroperoxide, problems in data acquisition were encountered due both to the low solubility of cumene hydroperoxide and the interference of absorbance changes from destruction of the enzyme (see below).

Biphasic Absorbance Changes—Fig. 2*A* illustrates the typical biphasic behavior observed when P-450$_{LM_2}$ was mixed with different concentrations of *m*-bromobenzyl hydroperoxide. Each kinetic trace obtained with *m*-bromobenzyl hydroperoxide could be described mathematically as a sum of two exponential functions of time:

$$\Delta A_t = \Delta A_f e^{-k_f t} + \Delta A_s e^{-k_s t} \qquad (12)$$

where ΔA_t and t are defined as in Equation 1, ΔA_f and ΔA_s are the total absorbance changes associated with the first and second phases, respectively, and k_f and k_s are the observed first order rate constants corresponding to the first and second phases, respectively. Each kinetic trace was analyzed initially with a semilogarithmic plot of ΔA_t *versus* time (33). Although curved near the ordinate, this plot became linear when only the second exponential process was significant. The slope and extrapolated ordinate intercept of this linear portion yielded values of k_s and ΔA_s, respectively. Values for ΔA_f and k_f were then determined from the ordinate intercept and slope, respectively, of a semilogarithmic plot of $(\Delta A_t - \Delta A_s e^{-k_s t})$ *versus* time. These values were then used in the subsequent secondary plots.

The total absorbance change at the end of the biphasic reaction, ΔA_∞, is the sum of the absorbance changes due to each phase, $\Delta A_f + \Delta A_s$. Fig. 2*B* shows the dependence of ΔA_∞ upon the concentration of *m*-bromobenzyl hydroperoxide. Note that this concentration dependence appears hyperbolic, just as it did with cumene hydroperoxide, and does not resemble a stoichiometric titration of the P-450 with the peroxy compound. A value of $K_d = 26$ μM was obtained from a linear Benesi-Hildebrand plot of the data in the same manner as described above for the cumene hydroperoxide example.

The values of both k_f and k_s were complex functions of the *m*-bromobenzyl hydroperoxide concentration; the value of k_f was a nonlinear, concave-up function of the hydroperoxide concentration, while the value of k_s was a nonlinear, concave-

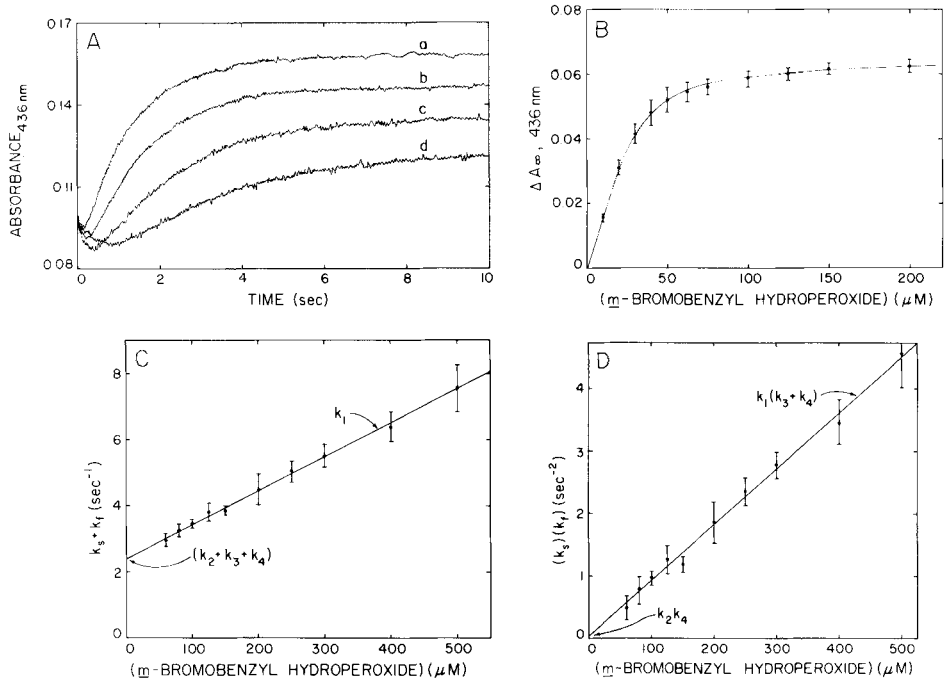

FIG. 2. **Calculation of rate constants when the kinetic traces were biphasic.** *A*, shows representative stopped flow kinetic traces observed at 436 nm after P-450$_{LM_2}$ was mixed with different concentrations of *m*-bromobenzyl hydroperoxide. The P-450$_{LM_2}$ concentration after mixing was 2.8 μM and that of the *m*-bromobenzyl hydroperoxides was 200, 50, 20, and 10 μM in Experiments *a* through *d*. *B*, shows the dependence of the total absorbance change, ΔA_∞, at 436 nm upon the final concentration of *m*-bromobenzyl hydroperoxide. The absorbance changes in *A* and *B* are those observed with a 2-cm optical path length. *C* and *D*, show the dependencies of the sum and the product, respectively, of the rate constants for the first phase (k_f) and the second phase (k_s) of the absorbance change at 436 nm upon the final concentration of *m*-bromobenzyl hydroperoxide. The values of k_f, k_s, and ΔA_∞ were obtained as described in the text. Each *error bar* in *B*, *C*, and *D* represents the standard deviation of four determinations. The values of the ordinate intercepts and slopes of the linear plots in both panels were obtained from linear regression analyses. These values were then used to calculate the values for the rate constants as listed in Table I.

down function of the hydroperoxide concentration. Both functions extrapolated to positive values at a *m*-bromobenzyl hydroperoxide concentration of zero. The fact that k_f increases as the concentration of hydroperoxide is raised, while k_s appears to eventually approach a constant value, suggests the occurrence of a bimolecular reaction coupled to a unimolecular reaction; thus, the simplest mechanism consistent with this behavior is again that of Equation 7.

Since the kinetic traces are clearly biphasic, the approach taken with the cumene hydroperoxide data is not applicable. If the rate equations are linear, the values for the time constants (k_f and k_s) associated with the mechanism of Equation 7 can be obtained by solving the determinant given in Equation 13 (34, 35).

$$\begin{vmatrix} k_1(\mathrm{B}) + k_2 - \lambda_i & -k_2 \\ -k_3 & k_3 + k_4 - \lambda_i \end{vmatrix} = 0 \qquad (13)$$

where the λ_i's, the eigenvalues of the matrix, are the solutions required to fulfill the equality and (B) is the concentration of the peroxy compound. In general, the concentration of B should be replaced by the sum of the equilbrium concentrations of free B and free P-450, but the above formulation is sufficient under pseudo-first order conditions. Equation 13 has two eigenvalues which correspond to the two time constants observed experimentally, k_f and k_s. Each eigenvalue expresses an observed time constant as a function of the individual rate constants of the mechanism in Equation 7. However, the two solutions of the quadratic equation which define the two time constants are sufficiently intractable so as to make direct calculation of the individual rate constants from the experimentally observed time constants unfeasible. Fortunately, two relationships exist in a two-dimensional matrix between the elements and the eigenvalues (36, 37); the sum of the two eigenvalues is equal to the trace of the matrix (Equation 14),

$$k_f + k_s = k_1(\mathrm{B}) + k_2 + k_3 + k_4 \qquad (14)$$

and the product of the two eigenvalues is equal to the determinant of the matrix (Equation 15),

$$k_f k_s = k_1(\mathrm{B})(k_3 + k_4) + k_2 k_4 \qquad (15)$$

Equations 14 and 15 predict that both the sum and the product of the two observed rate constants will be linear functions of the *m*-bromobenzyl hydroperoxide concentration. These plots are shown in Fig. 2, *C* and *D*, respectively. The values of the slopes and intercepts of the linear plots in Fig. 2, *C* and *D*, are defined as shown in the figures; with four equations and four unknowns, all of the individual rate constants of Equation 7 can be calculated (k_1 = 1000 $\mathrm{M^{-1}s^{-1}}$, k_2 = 1.53 $\mathrm{s^{-1}}$, k_3 = 0.87 $\mathrm{s^{-1}}$, and k_4 = 0.015 $\mathrm{s^{-1}}$).

The behavior observed when P-450$_{LM_2}$ is exposed to *m*-bromobenzyl hydroperoxide can thus be characterized mathematically by the same mechanism which accounted for the cumene hydroperoxide behavior. Although the reaction of either compound with P-450 follows the mechanism in Equation 7, whether the experimental kinetic traces will appear to be pseudo-first order or biphasic is governed by the values of the individual rate constants, the concentration of the peroxy compound, and the dead time of the stopped flow spectrophotometer. In the cumene hydroperoxide case, the fact that $k_2 \gg k_3$ led to the two phases being well separated on the time axis such that only glimpses of the first phase could be obtained. When k_2 is comparable in magnitude to k_3, as with

m-bromobenzyl hydroperoxide, there are two consequences: (*a*) the two phases are no longer well separated on the time axis, and (*b*) the transient concentration of Complex C will be higher than in the rapid equilibrium case. The combination of these two consequences, therefore, permits facile observation of both phases of the reaction. Note, however, that even though the transient concentration of Complex C is much higher in this case, the values of k_3 and k_4 dictate that the final equilibrium mixture will still contain predominantly Complex D and native P-450.

Effects of pH—Since many of the peroxy compounds used in these studies have pK_a values in the range of 7.0 to 8.0, the rate of Complex D formation was studied as a function of pH to determine whether the P-450 shows a preference for the ionized or unionized form of the peroxy compound. The pseudo-first order rate constant for the formation of Complex D with cumene hydroperoxide was invariant over the pH range of 5.0 to 9.0, as illustrated in Fig. 3; the same results were obtained with benzyl hydroperoxide (not shown). Since cumene hydroperoxide and benzyl hydroperoxide have pK_a values of around 12.0, these observations indicate that ionization of groups on the enzyme over the pH range studied had no significant influence on k_{obs}. In contrast, the k_{obs} for the formation of Complex D with various perbenzoic acids decreased markedly with increasing pH in this range. Fig. 3 shows the dependence of k_{obs} upon pH observed with three representative perbenzoic acids and also indicates the respective pK_a values. The close correspondence between the midpoint of each experimental curve and the pK_a of the peracid indicates that it is predominantly the unionized form which reacts with the enzyme. The same behavior was also observed with unsubstituted perbenzoic acid and with the *m*-nitro- and *p*-methyl-substituted derivatives (data not shown). Since the majority of the stopped flow experiments in this paper were performed at pH 7.0, the k_{obs} for Complex D formation could

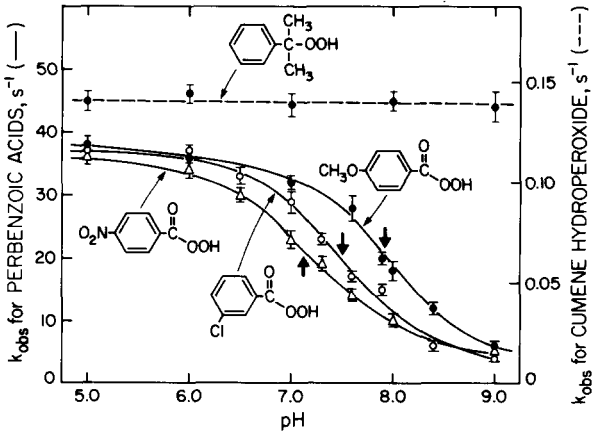

FIG. 3. **Effect of pH on the pseudo-first order rate constant for formation of Complex D.** The concentrations of P-450$_{LM_2}$ and dilauroyl-GPC were 2.7 μM and 50 μg per ml, respectively, after mixing, and those of the peroxy compounds were as follows: cumene hydroperoxide, 1.0 mM; *p*-nitroperbenzoic acid, 150 μM; *m*-chloroperbenzoic acid, 150 μM; and *p*-methoxyperbenzoic acid, 300 μM. The P-450$_{LM_2}$ and the peroxy compound were prepared in the appropriate buffer and added to separate syringes of the stopped flow spectrophotometer. The buffers used were as follows: pH 5.0, 0.10 M sodium citrate; pH 6.0 to 7.6, 0.05 M sodium phosphate; and pH 7.9 to 9.0, 0.05 M sodium pyrophosphate. The pH of each buffer was adjusted at 10°C, the temperature at which the experiments were performed. The values of k_{obs} obtained with the *p*-nitro- and *p*-methoxyperbenzoic acids were multiplied by 10 and 20, respectively, in order to facilitate comparison of the curves. The *bold arrows* indicate the pK_a values of the perbenzoic acids.

be corrected quite easily for the degree of ionization of the perbenzoic acid (38–40). Published values for the pK_a values of the perbenzoic acids were used for these corrections, or if the value was not known it was calculated from the empirical relationship:

$$pK_a \text{ (perbenzoic acid)} = 0.673\ pK_a \text{ (benzoic acid)} + 4.875 \quad (16)$$

Linear Free Energy Relationships—The two treatments of the primary kinetic data described above were successfully applied to every aromatic peroxy compound which gave either pseudo-first order or biphasic kinetic traces when mixed with P-450$_{LM_2}$. A complete list of these peroxy compounds, along with their respective kinetic and equilibrium constants, is included in Table I. Where appropriate, the values have been corrected for pH effects, as described above. In all cases, the observed kinetic behavior could be adequately described by the two-step reversible mechanism represented in Equation 7. One consequence of this apparently reversible mechanism is that none of the peroxy compounds appear to titrate the P-450 stoichiometrically. Instead, the interaction between the P-450 and the peroxy compound can be characterized by the apparent dissociation constant, K_d, which is defined as k_2k_4/k_1k_3. The K_d values determined from spectral titrations such as those shown in Figs. 1*B* and 2*B* agree quite well with those calculated from the individual rate constants determined from secondary kinetic plots such as shown in Figs. 1, *C* and *D*, and 2, *C* and *D*.

Several structure-activity relationships became apparent from the values of the macroconstants, K_d and k_{obs}. For example, the value of K_d decreased by roughly 3-fold for each additional methylene group in the series of *p*-alkylperbenzoic acids (Table I). This observation suggested that hydrophobic bonding might be a factor in the overall formation of Complex D. The dependence of the logarithm of the ratio k_2/k_1 upon the Hansch π value is shown in Fig. 4 for each class of aromatic peroxy compound studied. The ratio k_2/k_1 is the dissociation constant for the first equilibrium. The value of π is a unitless parameter defined as $\log P_x - \log P_H$, where P_H is the partition coefficient of a parent molecule (substituent = H) between 1-octanol and water and P_x is the partition coefficient for the substituted molecule (41). The value of π is thus a measure of the effect of the substituent upon the lipophilicity of the compound. A positive π value signifies that the substituent increases the lipophilicity of the compound, while a negative π value signifies that the substituent decreases the lipophilicity of the compound. The greater the magnitude of π, the greater is the effect. It is clear from Fig. 4 that, the more lipophilic the substituted peroxy compound, the more tightly it appears to bind to the P-450. The following relationships were obtained from a linear regression analysis of each plot in Fig. 4. For benzyl hydroperoxides, $\log k_2/k_1 = -1.02\ \pi - 1.762$, $n = 12$, and $r = 0.990$; for cumene hydroperoxides, $\log k_2/k_1 = -1.04\ \pi - 1.993$, $n = 6$, and $r = 0.990$; and for perbenzoic acids, $\log k_2/k_1 = -0.99\ \pi - 2.433$, $n = 17$, and $r = 0.997$, where n is the number of points and r is the correlation coefficient. The slopes of all three plots are equal to unity. This indicates that substitution of the aromatic ring of the peroxy compound has exactly the same effect on the free energy of binding the peroxy compound to P-450$_{LM_2}$ as on the free energy of transferring an organic compound from an aqueous phase to 1-octanol. Thus, the various functional groups (nitro, cyano, *n*-propyl, methoxy, etc.) do not appear to play special roles in the first equilibrium other than their influence on the π values derived from the 1-octanol-water model. Furthermore, the ordinate intercepts of all three plots are ranked in the same order as the partition coefficients of the parent organic compounds (41). Both observations indi-

TABLE I

Kinetic constants obtained with substituted peroxy compounds

The values of K_d were obtained from Equation 6, and the values of k_2/k_1, k_3, and k_4 were obtained from kinetic plots as described in the text. When k_2 was less than 150 s^{-1}, the values of k_1 and k_2 were obtained directly using Equation 11. When k_2 was greater than 150 s^{-1}, these values were calculated as described in the text.

Substituent	K_d	k_2/k_1	$k_1 \times 10^{-3}$	k_2	k_3	k_4	π[a]	σ
	μM	mM	$M^{-1}s^{-1}$	s^{-1}	s^{-1}	s^{-1}		
Perbenzoic acids								
p-$CH_3CH_2CH_2$	4.0	0.14	440	62	52	1.5	1.42[b]	−0.151[c]
p-Br	5.4	0.44	1100	480	150	1.8	0.98	0.232
p-CH_3CH_2	12	0.42	230	97	41	1.2	0.92[b]	−0.151
p-Cl	6.5	0.57	230	130	110	1.3	0.87	0.227
m-Cl	6.4	0.55	950	520	210	2.4	0.83	0.373
m-CH_3CH_2O	9.7	0.97	670	650	96	0.96	0.64[b]	0.100
p-CH_3CH_2O	10	0.91	430	390	38	0.42	0.58[b]	−0.240
m-CH_3	11	1.1	220	240	60	0.60	0.52	−0.069
p-CH_3	17	1.4	120	170	41	0.50	0.42	−0.170
m-F	15	2.0	220	440	150	1.1	0.28	0.337
p-F	10	2.1	270	560	110	0.51	0.19	0.062
m-CH_3O	22	3.0	150	460	110	0.89	0.14	0.115
p-CH_3O	19	3.2	94	300	31	0.19	0.08	−0.268
p-NO_2	18	3.1	320	980	110	0.64	0.02	0.778
H	16	3.9	79	310	70	0.28	0	0
m-NO_2	7.8	4.5	240	1100	390	0.67	−0.05	0.710
p-CN	40	7.2	46	330	82	0.45	−0.31	0.660
o-CH_3	38	1.8	67	120	39	0.83		
o-Cl	6.2	0.61	340	210	98	1.0		
Cumene hydroperoxides								
p-Cl	26	1.3	52	67	8.3	0.18	0.86	0.227
m-CH_3	53	3.3	6.4	21	0.81	0.013	0.50	−0.069
p-CH_3	48	3.0	15	45	0.49	0.0075	0.48	−0.170
m-F	68	3.9	28	110	15	0.26	0.33	0.337
p-F	65	6.7	18	120	2.2	0.022	0.22	0.062
H	73	10	5.0	50	1.5	0.011	0	0
Benzyl hydroperoxides								
p-Br	13	0.79	4.6	3.6	0.25	0.0040	1.19	0.232
m-Br	25	1.5	1.0	1.5	0.87	0.015	1.16	0.391
m-Cl	29	2.5	0.64	1.6	0.63	0.0067	0.84	0.373
m-CH_3	92	5.8	0.019	0.11	0.031	0.0005	0.50	−0.069
p-CH_3	180	5.5	0.006	0.033	0.015	0.0005	0.48	−0.170
m-F	270	7.8	0.11	0.83	0.49	0.017	0.33	0.337
p-F	310	10	0.016	0.16	0.071	0.0022	0.22	0.062
p-NO_2	89	13	0.85	11	1.4	0.0093	0.16	0.778
m-NO_2	160	11	1.0	11	5.2	0.075	0.11	0.710
p-CN	220	17	0.49	8.4	0.48	0.0063	0.03	0.660
H	340	19	0.041	0.78	0.033	0.0006	0	0
m-CN	83	16	0.62	9.9	2.1	0.011	0	0.560

[a] The π values for the perbenzoic acids are those published for the corresponding benzoic acids (41). The π values for the cumene and benzyl hydroperoxides are those published for the corresponding benzyl alcohols. Where a value of π for a particular substituent had not been reported for the corresponding benzyl alcohol, it was calculated from the relationship, $\pi_{\text{benzyl alcohol}} - \pi_n = 0.469\ \sigma + 0.041$, where π_n is the π value for substituted benzene (41).

[b] These values of π were obtained by adding 0.50 for each additional methylene group to the corresponding methoxy or methyl substituents.

[c] This value of σ was assumed to be the same as that of the *p*-ethyl substituent.

cate that the first equilibrium of Equation 7 is driven primarily by hydrophobic bonding.

The existence of another structure-activity relationship was suggested by the observation that within each congeneric series of peroxy compounds the k_{obs} for Complex D formation was, in general, a function of the electron-donating or withdrawing tendency of the substituent. Accordingly, the dependence of the logarithm of k_3 upon the Hammett σ value is shown in Fig. 5 for each class of aromatic peroxy compound. The rate constant k_3 is the constant for the conversion of Complex C to Complex D. The value of σ is a unitless parameter defined as $\rho\sigma = \log K_x - \log K_H$, where K_H is the equilibrium or rate constant of a parent molecule (substituent = *H*) and K_x is that for the substituted molecule (42). The value of ρ is a number characteristic of the reaction, whereas σ is a number characteristic of the substituent. The value of ρ is defined as unity for the ionization of benzoic acids in water at 25°C; thus, the σ values are given directly as the pK_a of benzoic acid minus that of the substituted benzoic acid. A negative σ value is obtained with an electron-donating substituent, while a positive value is obtained with an electron-withdrawing substituent. The greater the magnitude of σ, the greater is the effect of the substituent. The following relationships were obtained from a linear regression analysis of each plot in Fig. 5. For perbenzoic acids, $\log k_3 = 1.12\ \sigma + 1.849$, $n = 15$, and $r = 0.984$; for cumene hydroperoxides, $\log k_3 = 3.05\sigma + 0.172$, $n = 6$, and $r = 0.998$; and for benzyl hydroperoxides, $\log k_3 = 2.99\ \sigma - 1.337$, $n = 10$, and $r = 0.997$. The points corresponding to the *p*-nitro and *p*-cyano derivatives of perbenzoic acid and benzyl hydroperoxide were omitted in the above calculations, as they clearly deviated from the line established by the other derivatives (Fig. 5). These two substituents frequently show deviations in linear free energy correlations (43). The correlation coefficients obtained with Hammett's σ values were far superior to those obtained from attempted fits to the appropriate σ^+ (44) or σ^- (45) values. All of the ρ values are positive, which indicates that the substituents exert the same type of influence upon the conversion of

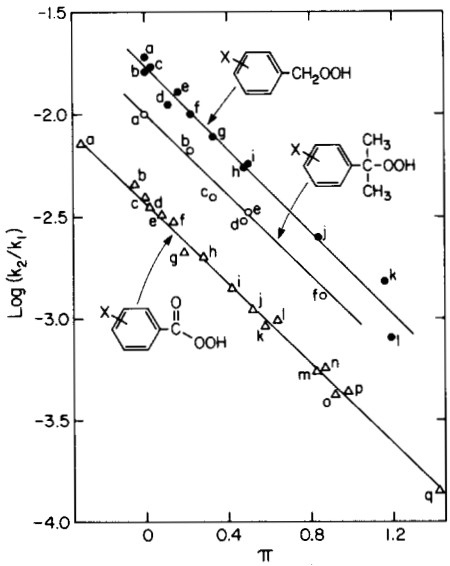

FIG. 4. **Dependence of the logarithm of k_2/k_1 upon the Hansch π value.** The ratio k_2/k_1 represents the dissociation constant for Complex C into free P-450$_{LM_2}$ and free peroxy compound. The ratios and the π values are those listed in Table I. Benzyl hydroperoxides: *a*, unsubstituted; *b*, *m*-cyano-; *c*, *p*-cyano-; *d*, *m*-nitro-; *e*, *p*-nitro-; *f*, *p*-fluoro-; *g*, *m*-fluoro-; *h*, *p*-methyl-; *i*, *m*-methyl-; *j*, *m*-chloro-; *k*, *m*-bromo-; and *l*, *p*-bromo-. Cumene hydroperoxides: *a*, unsubstituted; *b*, *p*-fluoro-; *c*, *m*-fluoro-; *d*, *p*-methyl-; *e*, *m*-methyl-; and *f*, *p*-chloro-. Perbenzoic acids: *a*, *p*-cyano-; *b*, *m*-nitro-; *c*, unsubstituted; *d*, *p*-nitro-; *e*, *p*-methoxy-; *f*, *m*-methoxy-; *g*, *p*-fluoro-; *h*, *m*-fluoro-; *i*, *p*-methyl-; *j*, *m*-methyl-; *k*, *p*-ethoxy-; *l*, *m*-ethoxy-; *m*, *m*-chloro-; *n*, *p*-chloro-; *o*, *p*-ethyl-; *p*, *p*-bromo-; and *q*, *p*-*n*-propyl-.

Complex C to Complex D as they do upon the ionization of benzoic acid. This may indicate that considerable negative charge is stabilized by the aromatic ring of the peroxy compound in the transition state between Complex C and Complex D.

Destruction of the Enzyme—The results presented thus far have dealt exclusively with the formation of Complexes C and D and have ignored any subsequent spectral changes. Following the formation of Complex D, the absorbance of the P-450 slowly decreased with time at all wavelengths. When the peroxy compound was in sufficient excess to the protein, virtually the entire absorbance of the heme was eventually bleached. This loss in absorbance was attributed to irreversible oxidation of the protoporphyrin IX group by these strong oxidizing agents. Although the kinetics of this destruction process were quite complex, the loss in absorbance could frequently be approximated as a first order process equal to $\Delta A_{des}e^{-k_{des}t}$, where ΔA_{des} is the change in absorbance due to destruction, and k_{des} is the pseudo-first order rate constant for the absorbance loss. Thus, a complete mathematical description of the formation of Complex D requires this additional exponential function of time. However, since the values of k_{des} were typically only 2 to 5% of those for Complex D formation regardless of whether a peracid or a hydroperoxide was added to the P-450, the absorbance changes represented by the above exponential term were not a significant detriment to monitoring Complex D formation unless the value of ΔA_{des} was quite large. In general, the effect of the destruction of the heme upon Complex D formation could be conveniently ignored until the concentration of the peroxy compound reached roughly 30 to 100 times the apparent K_d value of the peroxy compound with the P-450. Above this concentration range, the values of ΔA_∞ for Complex D formation began to decrease as the concentration of the peroxy compound increased. Although the presence of phospholipid did not affect the rate or extent of the absorbance change due to destruction, it had a dramatic effect in preventing precipitation of the protein as the heme absorbance disappeared.

Spectra of Complexes C and D—In principle, if the concentration of each enzyme species is known as a function of time during the course of a reaction, the spectrum of each can be constructed from a study of the kinetic traces obtained at multiple wavelengths. In order to calculate the concentration of each enzyme species at any time during a reaction, one must know (*a*) the apparent kinetic mechanism of the reaction, (*b*) the general solution to the set of differential equations describing that mechanism, and (*c*) the values of all the individual rate constants in the reactions. Fortunately, the general solution to Equation 13 representing the mechanism in Equation 7 can be obtained under pseudo-first order conditions (46) and takes the form:

$$(A)_i = C_{i1} + C_{i2}e^{-\lambda_1 t} + C_{i3}e^{-\lambda_2 t} \quad (17)$$

where $(A)_i$ is the concentration of the *i*th enzyme species, λ_1 and λ_2 are the two time constants for the mechanism, and C_{i1}, C_{i2}, etc., are constants particular to the *i*th enzyme species. Both the time constants and the C_i's are very complex functions of the individual rate constants, $k_1(B)$, k_2, k_3, and k_4 (46). Since these rate constants are known for the reaction of P-450 with each peroxy compound, all of the constants in Equation 17 can be calculated. Consequently, the concentration of each enzyme species, including native P-450, Complex C, and Complex D, can be calculated as a function of time for any concentration of any peroxy compound.

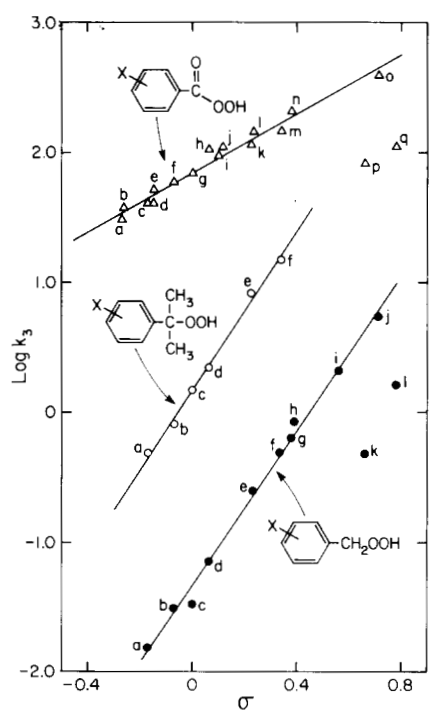

FIG. 5. **Dependence of the logarithm of k_3, the rate constant for conversion of Complex C to Complex D, upon the Hammett σ value.** The rate constants and the σ values are those listed in Table I. Perbenzoic acids: *a*, *p*-methoxy-; *b*, *p*-ethoxy-; *c*, *p*-methyl-; *d*, *p*-ethyl-; *e*, *p*-*n*-propyl-; *f*, *m*-methyl-; *g*, unsubstituted; *h*, *p*-fluoro-; *i*, *m*-ethoxy-; *j*, *m*-methoxy-; *k*, *p*-chloro-; *l*, *p*-bromo-; *m*, *m*-fluoro-; *n*, *m*-chloro-; *o*, *m*-nitro-; *p*, *p*-cyano-; and *q*, *p*-nitro-. Cumene hydroperoxides: *a*, *p*-methyl-; *b*, *m*-methyl-; *c*, unsubstituted; *d*, *p*-fluoro-; *e*, *p*-chloro-; and *f*, *m*-fluoro-. Benzyl hydroperoxides: *a*, *p*-methyl-; *b*, *m*-methyl-; *c*, unsubstituted; *d*, *p*-fluoro-; *e*, *p*-bromo-; *f*, *m*-fluoro-; *g*, *m*-chloro-; *h*, *m*-bromo-; *i*, *m*-cyano-; *j*, *m*-nitro-; *k*, *p*-cyano-; and *l*, *p*-nitro-.

These calculated concentrations can now be related to the experimentally observed absorbance. The total absorbance at any time can be described by a Beer's law combination of the molar absorptivities multiplied by the concentrations of the three species, as follows:

$$\text{absorbance} = \epsilon_{P\text{-}450}\,(\text{P-450}) + \epsilon_C\,(\text{Complex C}) + \epsilon_D\,(\text{Complex D}) \quad (18)$$

where ϵ_i is the absorption coefficient of the ith enzyme species. At the pseudo-equilibrium where the concentration of Complex D is maximal and destruction of P-450 is minimal, the predominant enzyme species are native P-450 and Complex D. Since $k_3 \gg k_4$ for all of the peroxy compounds in Table I, the concentration of Complex C is always negligibly small at equilibrium. If the absorption coefficient of Complex C is not orders of magnitude greater than the absorption coefficients of P-450 and Complex D, the ϵ_C (Complex C) term in Equation 18 may be neglected at equilibrium. The experimentally observed quantity, ΔA_∞, can, therefore, be expressed as $\Delta A_\infty = \Delta\epsilon_D$ (Complex D), where $\Delta\epsilon_D$ is $\epsilon_D - \epsilon_{P\text{-}450}$, the difference in absorption coefficients between Complex D and native P-450. The difference spectra of Complex D observed in the presence of three representative benzyl hydroperoxides and three representative perbenzoic acids are presented in Fig. 6, *A* and *B*, respectively. The lefthand ordinate shows the observed values of ΔA_∞ obtained at each wavelength examined. Whether the initial kinetic traces were mono- or biphasic, the calculated rate constants were independent of wavelength. The concentration of each peroxy compound used in Fig. 6 was chosen so that each spectrum would represent 90% conversion of P-450 to Complex D at equilibrium; this was accomplished using Equation 17 and the rate constants of Table I to calculate the concentration of peroxy compound needed. Thus, the righthand ordinate shows the appropriate values of $\Delta\epsilon_D$ for each peroxy compound, from which the value of ϵ_D at each wavelength can easily be determined.

The difference spectra in Fig. 6 are certainly not identical. The isosbestic point between Complex D and native P-450 was shifted 9 nm by replacing the *p*-methyl substituent of benzyl hydroperoxide with a *m*-nitro group. In fact, each substituted benzyl hydroperoxide of the 12 studied produced a unique difference spectrum for Complex D. Similar observations were made with the substituted perbenzoic acids, although the differences were not as great. Several of the peracids (*p*-fluoro-, *m*-fluoro-, *p*-methyl-, and *m*-methyl-, as well as unsubstituted) produced Complex D's qualitatively similar to that of *p*-chloroperbenzoic acid as judged by isosbestic points and positions of the peaks and troughs; however, the magnitudes of the absorbance changes were unique to the peroxy compound, varying up to 3-fold between certain compounds. The difference spectra obtained with the six substituted cumene hydroperoxides showed a similar dependence upon the structure of the organic portion of the peroxy compound in experiments not shown. In general, an electron-withdrawing substituent induced a red shift in the peak of the difference spectrum and the position of the isosbestic point between Complex D and native P-450, while an electron-donating substituent induced a corresponding blue shift. The difference spectra of Complex D's obtained with the *o*-methyl- and *o*-chloroperbenzoic acids were not significantly different from those observed with the corresponding *m*- or *p*-substituted derivatives. The spectrum of the Complex D formed in the presence of *p*-methylbenzyl hydroperoxide was unaffected by the presence of *m*-nitrobenzyl alcohol, even when the concentration of the alcohol was in 10-fold molar excess to that of the hydroperoxide. Similarly, the spectrum of the Complex D formed in the presence of *m*-nitrobenzyl hydroperoxide was unaffected by the presence of an excess of *p*-methylbenzyl alcohol. The presence of various substituted benzoic acids also had no effect on the spectrum of the Complex D formed with a particular perbenzoic acid.

The difference spectrum of Complex C could be constructed from the biphasic kinetic traces observed with those peroxy compounds whose rate constants permitted a transient buildup of Complex C. At the time at which the concentration of Complex C reached its maximum (before decaying to a negligibly small concentration at equilibrium), the ϵ_C (Complex C) term in Equation 18 could not be neglected. Under these conditions, the experimentally observed quantity, ΔA_f (Equation 12), can be expressed as $\Delta A_f = \Delta\epsilon_C$ (Complex C) + $\Delta\epsilon_D$ (Complex D), where $\Delta\epsilon_C$ is $\epsilon_C - \epsilon_{P\text{-}450}$, the difference in absorption coefficient between Complex C and native P-450. Since the value of $\Delta\epsilon_D$ could be determined at equilibrium and the concentration of each enzyme species could be calculated

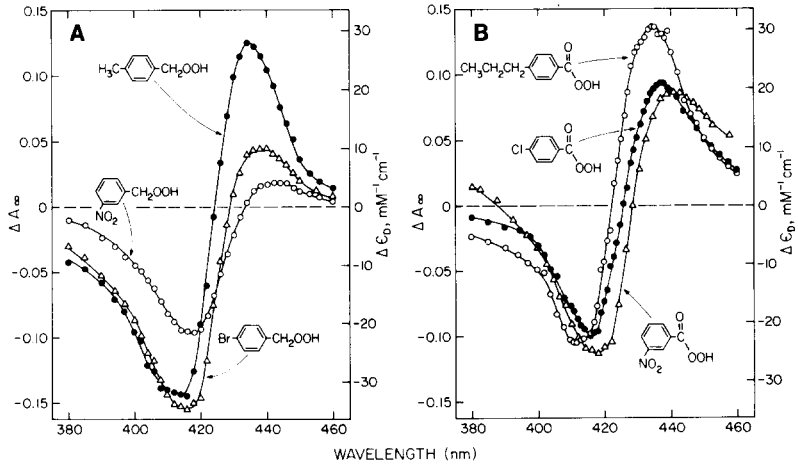

FIG. 6. **Difference spectrum of Complex D observed after mixing P-450$_{LM_2}$ and selected benzyl hydroperoxides (*A*) or perbenzoic acids (*B*), representing the absolute spectrum of Complex D minus that of native P-450$_{LM_2}$.** Each spectrum was constructed by analyzing separate kinetic traces at each of the wavelengths indicated. The absorbance differences are those observed with a 2-cm optical path length. The concentrations of the various components after mixing were as follows: P-450$_{LM_2}$, 2.4 μM; *p*-methylbenzyl hydroperoxide, 1.62 mM; *p*-bromobenzyl hydroperoxide, 117 μM; *m*-nitrobenzyl hydroperoxide, 1.45 mM; *p*-*n*-propylperbenzoic acid, 36 μM; *p*-chloroperbenzoic acid, 58 μM; and *m*-nitroperbenzoic acid, 70 μM. The concentration of each peroxy compound was carefully chosen so that each difference spectrum would represent approximately 90% conversion of P-450$_{LM_2}$ to Complex D.

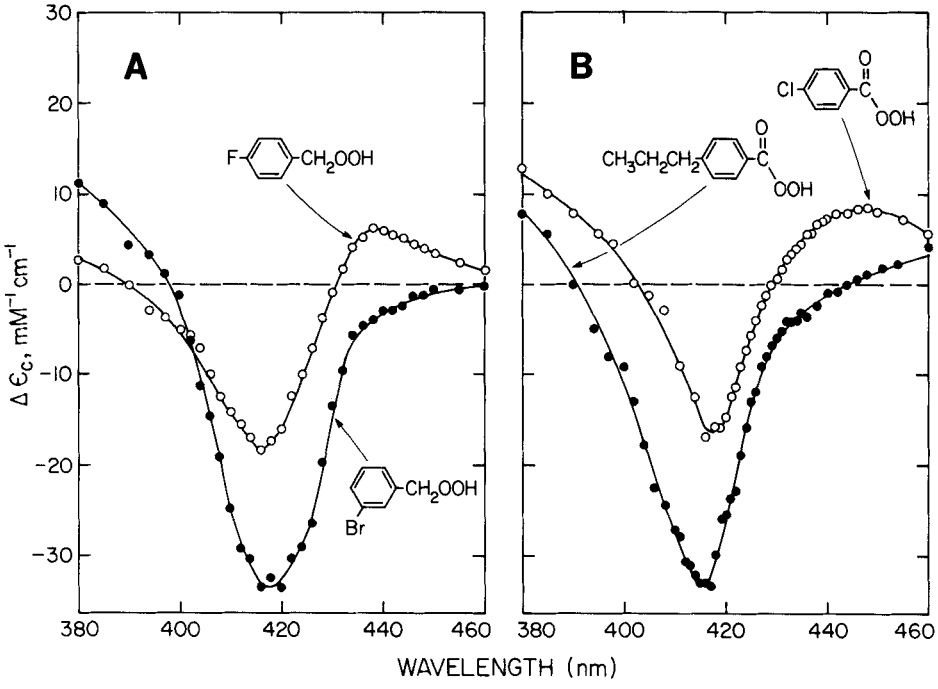

FIG. 7. **Difference spectra of Complex C's formed in the presence of two benzyl hydroperoxides (*A*) and perbenzoic acids (*B*), representing the absolute spectra of Complex C minus that of native P-450$_{LM_2}$.** Each spectrum was constructed by analyzing separate kinetic traces at each of the wavelengths indicated. The spectra were calculated as described in the text, each representing a hypothetical 100% conversion of P-450$_{LM_2}$ to Complex C.

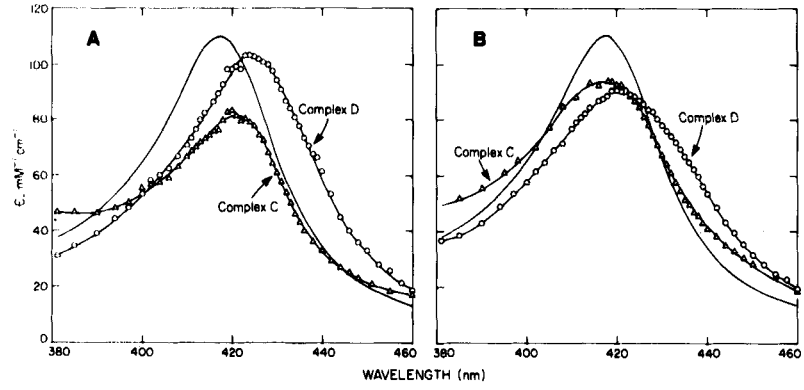

FIG. 8. **Absolute spectra of both Complex C and Complex D for two representative peroxy compounds.** The spectra were calculated as described in the text; each represents 100% of the P-450$_{LM_2}$. *A*, shows the spectra of native P-450 (——) and Complexes C (△——△) and D (○——○) formed in the presence of *p-n*-propylperbenzoic acid. *B*, shows the corresponding results with *p*-chloroperbenzoic acid.

at any time, the value of $\Delta\epsilon_C$ (and, therefore, ϵ_C) could easily be obtained as long as a reliable value of ΔA_f could be measured. The difference spectra of Complex C's observed in the presence of two representative benzyl hydroperoxides and two representative perbenzoic acids are presented in Fig. 7, *A* and *B*, respectively. Note that while these spectra are presented as $\Delta\epsilon_C$ values for a hypothetical 100% conversion of the P-450 to Complex C, only 10 to 30%, at best, of the P-450 is transiently converted to Complex C by any of the 37 aromatic peroxy compounds examined here. The difference spectrum of each Complex C shown in Fig. 7 is unique; this same observation was true for the spectrum of eight such complexes examined.

Since values for both ϵ_C and ϵ_D could be obtained for eight of the peroxy compounds, the absolute spectra of both species were plotted for each peroxy compound. The relationship of Complex D to Complex C fell into one of two general classes, depending upon the structure of the peroxy compound, as represented in Fig. 8. Fig. 8*A* shows the absolute spectra of Complexes C and D generated by mixing P-450$_{LM_2}$ with *p-n*-propylperbenzoic acid, while Fig. 8*B* shows the corresponding results with *p*-chloroperbenzoic acid. The Soret peak of Complex D was red shifted relative to that of Complex C with each peroxy compound, regardless of the substituent on the peroxy compound. In addition, the electronic properties of the substituent appeared to dictate whether the absorption coefficient of Complex D at its peak was higher or lower than that of Complex C at its peak. When the substituent was an electron-donating group, as in *p-n*-propylperbenzoic acid and *m*-methyl- or *p*-methylbenzyl hydroperoxide, the absorption coefficient of Complex D was higher than that of Complex C. On the other hand, when the substituent was an electron-withdrawing group, as in *p*-chloroperbenzoic acid and *m*-bromo-, *m*-fluoro-, *p*-fluoro-, or *m*-chlorobenzyl hydroperoxide, the absorption coefficient of Complex D was lower than that of Complex C. It should be noted that the isosbestic point between Complexes C and D in Fig. 8*A* is 401 nm, while that between Complexes C and D in Fig. 8*B* is 422 nm. Thus, the absolute spectra of the four species do not share a common isosbestic point. This observation, which was true for the absolute spectra of all the Complexes C and D examined, has important mechanistic implications.

DISCUSSION

The results presented here indicate that the reactions between P-450$_{LM_2}$ and a host of aromatic peroxy compounds do not conform to the peroxidase model shown in Equation 4. The reaction between a peroxidase and an appropriate peroxy compound to form Compound I has two obvious characteristics. First, since the formation of Compound I is essentially an

irreversible reaction, the peroxidase can be titrated with each peroxy compound to obtain a clear 1:1 stoichiometry for the reaction. Secondly, the spectral properties of the common iron-oxo intermediates resulting from the reaction of each peroxy compound are completely dependent upon the peroxidase used and independent of the nature of the peroxy compound. These observations have been reported for horseradish peroxidase (47), turnip peroxidase (40, 48), cytochrome *c* peroxidase (49), chloroperoxidase (50), catalase (51), and even for deuteroferriheme free in solution (52). In no instance has the reaction between P-450$_{LM_2}$ and any of forty aromatic peroxy compounds resulted in a stoichiometric titration, nor has the spectrum of the resulting intermediates been independent of the peroxy compound used. These discrepancies between the expected and the observed kinetic and spectral behavior can be accommodated by two explanations; one can either attach restrictions and exceptions to the peroxidase model of Equation 4 to force it to conform to the experimental observations obtained wth the P-450 system, or one can abandon the peroxidase model of P-450 action. These alternatives are considered below.

The dependence of the spectrum of each intermediate upon the structure of the peroxy compound is consistent with only one interpretation; the organic portion of the peroxy compound is retained in both Complex C and Complex D. It should be noted that the spectra of Complexes C and D do not represent different mixtures of Compound I and Compound II, which could be produced by reduction of Compound I by impurities in the enzyme preparation or the reagents. When known mixtures of Compounds I and II were generated by mixing impure horseradish peroxidase (R_z = 1.2) with a 10-fold excess of each of the three benzyl hydroperoxides used in Fig. 6*A*, a very clear isosbestic point between Compounds I and II was observed at 395 nm with all three peroxy compounds (data not shown). No such common isosbestic point can be found in the P-450 spectra shown here. Thus, to retain the oxenoid nature of the peroxidase intermediate of Equation 4 in the P-450 system, one must propose that the organic portion of the peroxy compound remains bound to the P-450 after heterolytic oxygen-oxygen bond breakage has occurred. While this proposition cannot be absolutely ruled out by the data presented here, the experiments showing that the presence of different benzyl alcohols does not affect the spectrum of the Complex D formed with a particular benzyl hydroperoxide require the further restriction to the model that the alcohol formed after oxygen-oxygen bond breakage not be exchangeable with the alcohol in the solution (at least, under the experimental conditions described). One additional shortcoming of the peroxidase model is the apparent reversibility observed for the formation of each intermediate with P-450.

Since a number of assumptions must be made to fit the peroxidase model to the observations obtained with P-450, it is worthwhile to briefly consider other models. One immediately apparent alternative to heterolytic cleavage of the oxygen-oxygen bond in the peroxy compound is homolytic cleavage of the oxygen-oxygen bond, as proposed by White and Coon (17). Homolytic cleavage of the peroxide evidently occurs when H_2O_2 or alkyl hydroperoxides are mixed with ferrimyoglobin (53, 54). Although the reaction between ferrimyoglobin and a peroxy compound is quite complex (55), the predominant products of this reaction appear to be an oxidized protein species equivalent to Compound II of the peroxidases and either a hydroxyl or an alkoxyl radical, depending upon the structure of the peroxy compound. Although this Compound II-like derivative of ferrimyoglobin is not formed with a 1:1 stoichiometry with each peroxy compound (perhaps due to the complexity of the reaction), the spectrum of this intermediate is once again independent of the structure of the peroxy compound used to form the intermediate (56). If a similar homolytic cleavage occurs during the formation of either spectral intermediate observed during the reaction of a peroxy compound with P-450, one must again rationalize the dependence of the spectrum upon the identity of the peroxy compound. Unfortunately, the information so far available does not enable us to deduce the chemical identity of these spectral intermediates.

The first equilibrium of Equation 7 is clearly driven by hydrophobic bonding. It is reasonable to argue that no bond-making or breaking steps subject to the electronic influence of the substituent on the aromatic ring are involved in this equilibrium, since the correlation of log k_2/k_1 to the π values would not be as faithfully observed. The existence of this linear free energy correlation also indicates that the value of k_2 represents a true dissociation rate. If the value of k_2 were actually a composite of the rate of dissociation of Complex C into free P-450 and peroxy compound and the rate of a hypothetical regeneration of native P-450 via some type of alternate pathway involving turnover of the peroxy compound, one would not expect to obtain the observed correlation. Complex C thus has the kinetic characteristics of a Michaelis complex formed between P-450 and the peroxy compound. However, it is apparent that something other than mere hydrophobic bonding of an organic molecule to P-450 occurs during the formation of Complex C, since the spectra of various Complex C's do not resemble typical Type I binding spectra (which is indicative of partial conversion of the P-450$_{LM_2}$ from low spin ferric to high spin ferric).

The clear correlation of the log of k_3 with Hammett's σ values suggest that the conversion of Complex C to Complex D involves a bond-making or breaking step that is strongly influenced by the electronic properties of the substituent on the aromatic ring. Whether this step involves heterolytic or homolytic oxygen-oxygen bond cleavage, or, alternatively, some as yet unidentified chemical process, is not apparent from these data. The question of whether this conversion is truly reversible is very important to understanding the underlying chemical process. The value of k_4 as derived from the kinetic plots is, rigorously, the sum of all the chemical processes that are involved in the conversion of Complex D to either Complex C or native P-450. Thus, a kinetic analysis alone cannot distinguish whether the value of k_4 represents only the rate constant for the reverse reaction of the chemical process defined by the rate constant k_3, or a summation of rate constants including those for a hypothetical turnover of Complex D to regenerate Complex C or native P-450. Explanations of such a hypothetical turnover could include either reduction of Complex D by another molecule of peroxy compound (57, 58), or by some "endogenous donor" as referred to in the peroxidase literature (59), or perhaps hydroxylation of an additional molecule of peroxy compound. All of these proposals require the consumption of peroxy compound during the approach of Complex D to equilibrium. Preliminary experiments using horseradish peroxidase and *o*-dianisidine to monitor the concentration of benzyl hydroperoxide before and after the formation of Complex D do not indicate an appreciable loss of oxidizing equivalents during the formation of Complex D. Thus, the value of k_4 appears to reflect predominantly the back reaction of the process defined by the rate constant, k_3. Studies are in progress to clarify the nature of the spectral intermediates which have been described.

Whatever the chemical identity of these intermediates, the failure to detect a classical peroxidase Compound I-like intermediate in these reactions raises a serious doubt whether a simple peroxidase-like mechanism applies to the hydroxyl-

ation reactions catalyzed by P-450$_{LM}$ with various oxidants. It should be noted that in using the data reported here to question the involvement of a peroxidase type of intermediate in the peroxide-dependent, P-450$_{LM_2}$-catalyzed hydroxylation reactions, it has been tacitly assumed that one or both of the two spectral intermediates described are somehow involved in the hydroxylation reaction and not merely intermediates on the pathway to destruction of the heme. In a preliminary communication we have reported that Complex C, not Complex D, is intimately involved in the cumene hydroperoxide-dependent hydroxylation of toluene to form benzyl alcohol (60). Stopped flow spectrophotometric studies in the presence of substrates are currently in progress to define the role of these spectral species in the hydroxylation reaction.

Acknowledgments—We are grateful to Dr. Ronald E. White for advice and assistance in the synthesis of peroxy compounds and for carrying out the nmr and ir analyses. We also thank Sylvia B. Dahl and Leonard W. Cooke for preparing P-450$_{LM_2}$ from rabbit liver microsomes.

REFERENCES

1. Blake, R. C., II, and Coon, M. J. (1979) *Fed. Proc.* **38,** 319
2. Coon, M. J., Blake, R. C., II, Oprian, D. D., and Ballou, D. P. (1979) *Acta Biol. Med. Ger.* **38,** 449–458
3. Lu, A. Y. H., and Coon, M. J. (1968) *J. Biol. Chem.* **243,** 1331–1332
4. Coon, M. J., and Lu, A. Y. H. (1969) in *Microsomes and Drug Oxidations* (Gillette, J. R., Conney, A. H., Cosmides, G. J., Estabrook, R. W., Fouts, J. R., and Mannering, G. J., eds) pp. 151–166, Academic Press, New York
5. Lu, A. Y. H., Junk, K. W., and Coon, M. J. (1969) *J. Biol. Chem.* **244,** 3714–3721
6. Strobel, H. W., Lu, A. Y. H., Heidema, J., and Coon, M. J. (1970) *J. Biol. Chem.* **245,** 4851–4854
7. Nordblom, G. D., and Coon, M. J. (1977) *Arch. Biochem. Biophys.* **180,** 343–347
8. Kadlubar, F. F., Morton, K. C., and Ziegler, D. M. (1973) *Biochem. Biophys. Res. Commun.* **54,** 1255–1261
9. Rahimtula, A. D., and O'Brien, P. J. (1974) *Biochem. Biophys. Res. Commun.* **60,** 440–447
10. Nordblom, G. D., White, R. E., and Coon, M. J. (1976) *Arch. Biochem. Biophys.* **175,** 524–533
11. Hrycay, E. G., Gustafsson, J.-Å., Ingelman-Sundberg, M., and Ernster, L. (1975) *Biochem. Biophys. Res. Commun.* **66,** 209–216
12. Lichtenberger, F., Nastainczyk, W., and Ullrich, V. (1976) *Biochem. Biophys. Res. Commun.* **70,** 939–946
13. Gustafsson, J.-Å., Rondahl, L., and Bergman, J. (1979) *Biochemistry* **18,** 865–870
14. Berg, A., Ingelman-Sundberg, M., and Gustafsson, J.-Å., (1979) *J. Biol. Chem.* **254,** 5264–5271
15. Sligar, S. G., Kenney, K. A., and Pearson, D. C. (1980) in *Oxidases and Related Redox Systems* (King, T. E., Mason, H. S., and Morrison, M. E., eds) Pergamon Press, Oxford, in press
16. Coon, M. J., and White, R. E. (1980) in *Dioxygen Binding and Activation by Metal Centers* (Spiro, T. G., ed) John Wiley and Sons, Inc., New York, in press
17. White, R. E., and Coon, M. J. (1980) *Annu. Rev. Biochem.* **49,** in press
18. Lichtenberger, F., and Ullrich, V. (1976) in *Microsomes and Drug Oxidations* (Ullrich, V., Roots, I., Hildebrandt, A., Estabrook, R. W., and Conney, A. H., eds) pp. 218–223, Pergamon Press, New York
19. Rahimtula, A. D., O'Brien, P. J., Hrycay, E. G., Peterson, J. A., and Estabrook, R. W. (1974) *Biochem. Biophys. Res. Commun.* **60,** 695–702
20. Hrycay, E. G., Gustafsson, J.-Å., Ingelman-Sundberg, M., and Ernster, L. (1976) *Eur. J. Biochem.* **61,** 43–52
21. van der Hoeven, T. A., Haugen, D. A., and Coon, M. J. (1974) *Biochem. Biophys. Res. Commun.* **60,** 569–575
22. Haugen, D. A., and Coon, M. J. (1976) *J. Biol. Chem.* **251,** 7929–7939
23. Coon, M. J., van der Hoeven, T. A., Dahl, S. B., and Haugen, D. A. (1978) *Methods Enzymol.* **52,** 109–117
24. McDonald, R. N., Steppel, R. N., and Dorsey, J. E. (1970) in *Organic Syntheses,* Vol. 50, pp. 15–18, John Wiley and Sons, Inc., New York
25. Silbert, L. S., Siegel, E., and Swern, D. (1962) *J. Org. Chem.* **27,** 1336–1342
26. Cookson, P. G., Davies, A. G., and Roberts, B. P. (1976) *J. Chem. Soc. Chem. Commun.* 1022–1023
27. Armstrong, G. P., Hall, R. H., and Quin, D. C. (1950) *J. Chem. Soc.* 666–670
28. Brown, H. C., Brady, J. D., Grayson, M., and Bonner, W. H. (1957) *J. Amer. Chem. Soc.* **79,** 1897–1903
29. Martin, A. J. (1960) in *Organic Analysis* (Mitchell, J., Jr., Kolthoff, I. M., Proskauer, E. S., and Weissberger, A., eds) Vol. 4, pp. 15–16, Interscience, New York
30. Benesi, H. A., and Hildebrand, J. H. (1949) *J. Amer. Chem. Soc.* **71,** 2703–2707
31. Strickland, S., Palmer, G., and Massey, V. (1975) *J. Biol. Chem.* **250,** 4048–4052
32. Frost, A. A., and Pearson, R. G. (1961) in *Kinetics and Mechanism,* 2nd Ed, p. 186, John Wiley and Sons, Inc. New York
33. French, T. C., and Hammes, G. G. (1969) *Methods Enzymol.* **16,** 3–30
34. Castellan, G. W. (1963) *Ber. Bunsen-Ges. Phys. Chem.* **67,** 898–908
35. Hammes, G. G., and Schimmel, P. R. (1966) *J. Phys. Chem.* **70,** 2319–2324
36. Haslam, J. L. (1972) *J. Phys. Chem.* **76,** 366–369
37. Hammes, G. G., and Haslam, J. L. (1968) *Biochemistry* **7,** 1519–1524
38. Jones, P., and Middlemiss, D. N. (1972) *Biochem. J.* **130,** 411–415
39. Davies, D. M., Jones, P., and Mantle, D. (1976) *Biochem. J.* **157,** 247–253
40. Job, D., and Jones, P. (1978) *Eur. J. Biochem.* **86,** 565–572
41. Fujita, T., Iwasa, J., and Hansch, C. (1964) *J. Amer. Chem. Soc.* **86,** 5175–5180
42. Hammett, L. P. (1940) *Physical Organic Chemistry,* pp. 184–229, McGraw-Hill, New York
43. Jaffe, H. H. (1953) *Chem. Rev.* **53,** 191–221
44. Okamoto, Y., and Brown, H. C. (1958) *J. Amer. Chem. Soc.* **80,** 4979–4987
45. Bordwell, F. G., and Cooper, G. D. (1952) *J. Amer. Chem. Soc.* **74,** 1058–1060
46. Matsen, F. A., and Franklin, J. L. (1950) *J. Amer. Chem. Soc.* **72,** 3337–3341
47. Schonbaum, G. R., and Lo, S. (1972) *J. Biol. Chem.* **247,** 3353–3360
48. Job, D., Ricard, J., and Dunford, H. B. (1977) *Arch. Biochem. Biophys.* **179,** 95–99
49. Yonetani, T. (1966) *J. Biol. Chem.* **241,** 2562–2571
50. Hager, L. P., Doubek, D. L., Silverstein, R. M., Lee, T. T., Thomas, J. A., Hargis, J. H., and Martin, J. C. (1973) in *Oxidases and Related Redox Systems* (King, T. E., Mason, H. S., and Morrison, M., eds) pp. 311–332, University Park Press, Baltimore
51. Schonbaum, G. R., and Chance, B. (1976) in *The Enzymes* (Boyer, P. D., ed) pp. 363–408, Academic Press, New York
52. Jones, P., Mantle, D., Davies, D. M., and Kelley, H. C. (1977) *Biochemistry* **16,** 3974–3978
53. George, P., and Irvine, D. H. (1952) *Biochem. J.* **52,** 511–517
54. George, P., and Irvine, D. H. (1954) *Biochem. J.* **58,** 188–195
55. Fox, J. B., Jr., Nicholas, R. A., Ackerman, S. A., and Surft, C. E. (1974) *Biochemistry* **13,** 5178–5186
56. Yonetani, T., and Schleyer, H. (1967) *J. Biol. Chem.* **242,** 1974–1979
57. O'Brien, P. J. (1978) *Pharmacol. Ther. Part A Chemother. Toxicol. Metab. Inhibitors* **2,** 517–536
58. Metelitza, D. I., Akhrem, A. A., Erjomin, A. N., Kissel, M. A., and Usanov, S. A. (1979) *Acta Biol. Med. Ger.* **38,** 511–518
59. Dunford, H. B., and Stillman, J. S. (1976) *Coor. Chem. Rev.* **19,** 187–251
60. Blake, R. C., II, and Coon, M. J. (1980) in *Microsomes, Drug Oxidations, and Chemical Carcinogenesis* (Coon, M. J., Conney, A. H., Estabrook, R. W., Gelboin, H. V., Gillette, J. R., and O'Brien, P. J., eds) Academic Press, New York, in press